Reconstructing the atomic number of cargo X-ray images using dual energy radiography

Peter Lalor

July 18, 2023

First, a brief history…

U.S. Congress passes the SAFE Port Act of 2006

SEC. 232. SCREENING AND SCANNING OF CARGO CONTAINERS.

The secretary shall ensure integrated scanning systems are fully deployed to **scan all containers entering the United States** before such containers arrive in the United States

— Public Law 109-347

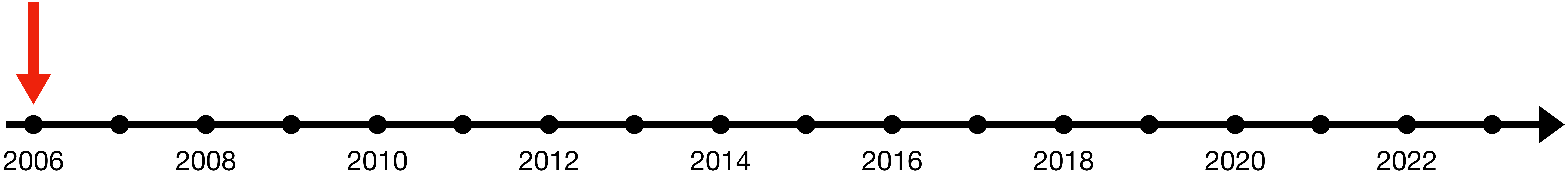

First, a brief history…

U.S. Congress passes the 9/11 Commission Act

Title XVII: Maritime Cargo

Modifies the SAFE Port Act to make this provision applicable to containers loaded in a foreign country **on or after July 1, 2012**

— Public Law 110-53

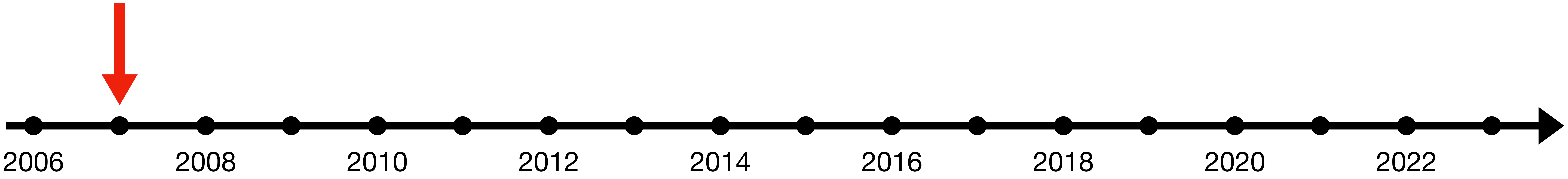

First, a brief history…

DHS secretary requests
a 2-year extension

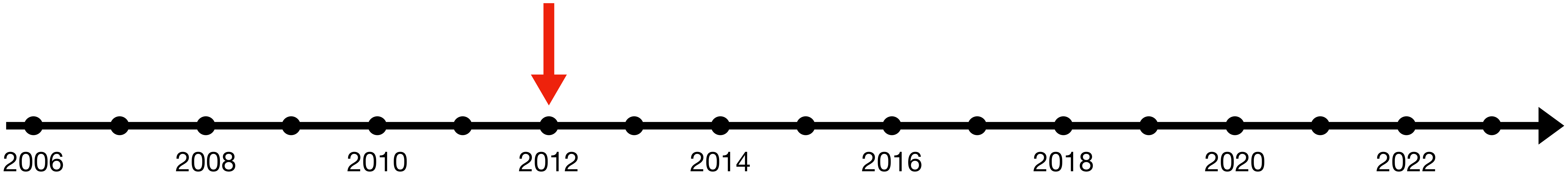

First, a brief history...

U.S. DEPARTMENT OF HOMELAND SECURITY

DHS secretary requests
a 2-year extension

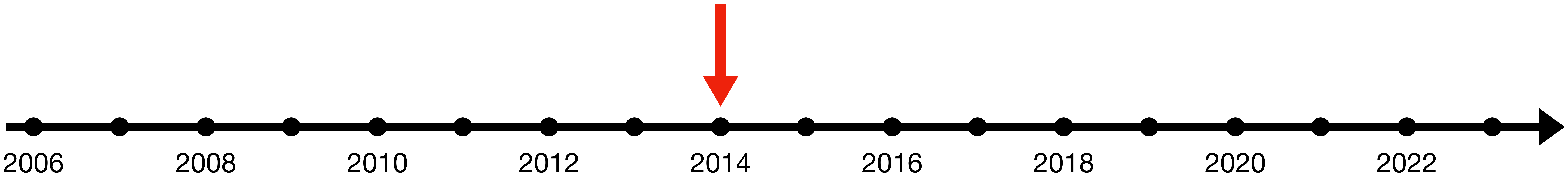

First, a brief history...

DHS secretary requests
a 2-year extension

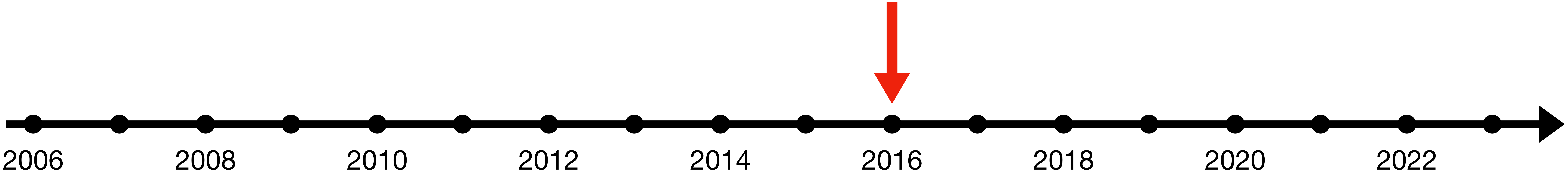

2006 2008 2010 2012 2014 2016 2018 2020 2022

First, a brief history…

DHS secretary requests
a 2-year extension

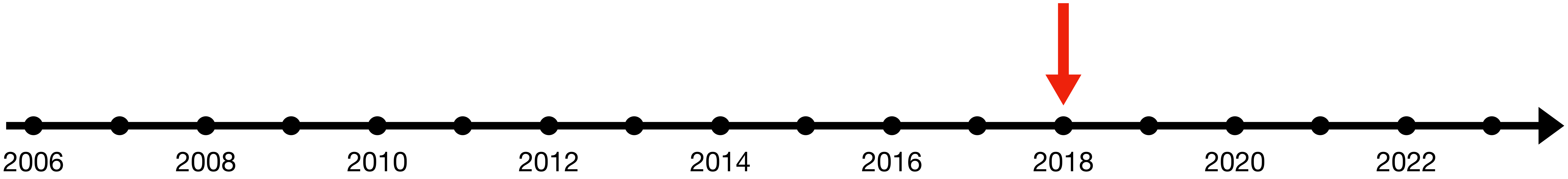

First, a brief history…

DHS secretary requests a 2-year extension

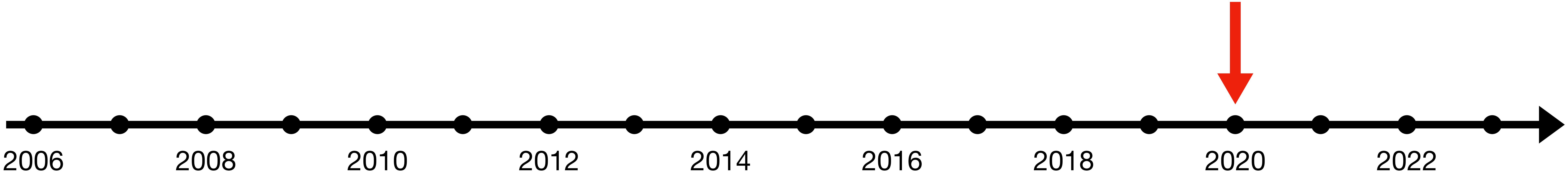

First, a brief history...

DHS secretary requests a 2-year extension

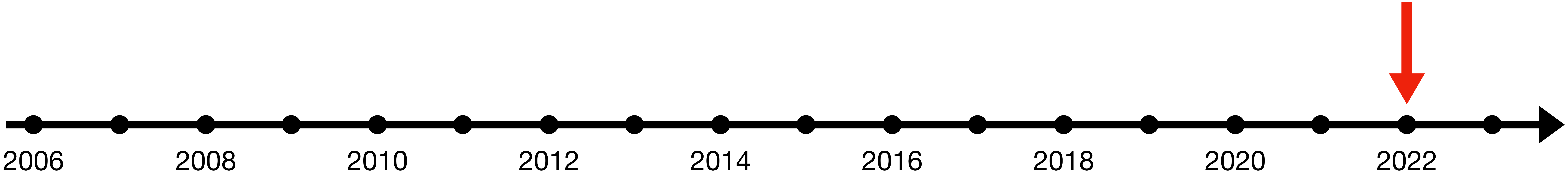

Why is the scanning requirement so elusive?

Source: "Scanning and Imaging Shipping Containers Overseas: Costs and Alternatives", CBO 2015

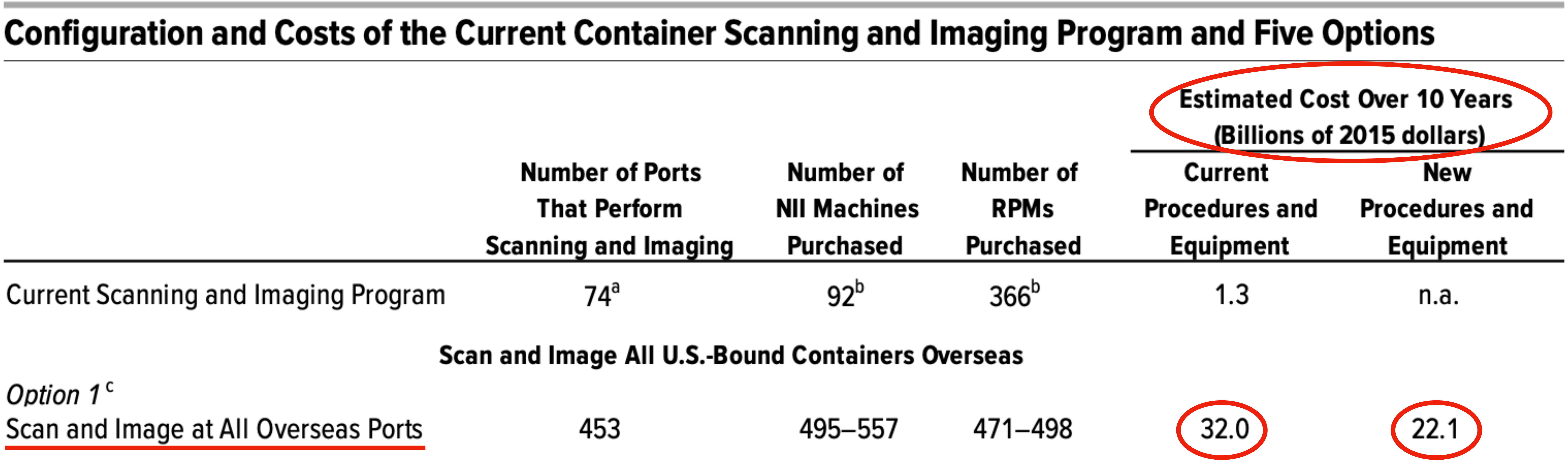

Configuration and Costs of the Current Container Scanning and Imaging Program and Five Options

				Estimated Cost Over 10 Years (Billions of 2015 dollars)	
	Number of Ports That Perform Scanning and Imaging	Number of NII Machines Purchased	Number of RPMs Purchased	Current Procedures and Equipment	New Procedures and Equipment
Current Scanning and Imaging Program	74[a]	92[b]	366[b]	1.3	n.a.
	Scan and Image All U.S.-Bound Containers Overseas				
Option 1[c] Scan and Image at All Overseas Ports	453	495–557	471–498	32.0	22.1

Installation and operational costs between $22 billion and $32 billion!

Research Overview

- Scanning systems need to have a **high detection rate** and **low false alarm rate**
- Currently: radiographic images are **manually reviewed** by **port operators**
- This work: **assist port operators by calculating the material composition of cargo contents**

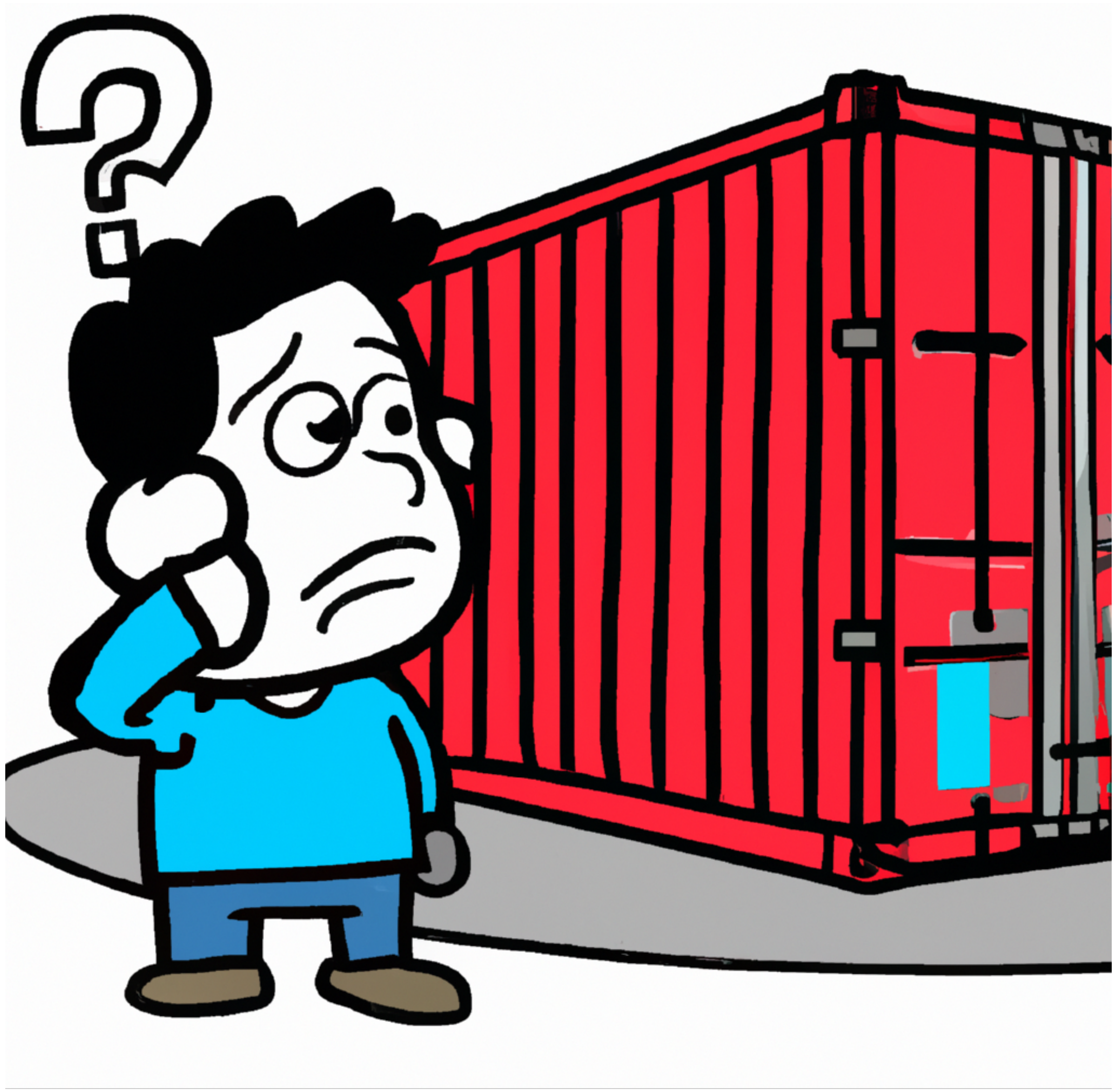

Radiography systems non-intrusively scan cargo containers

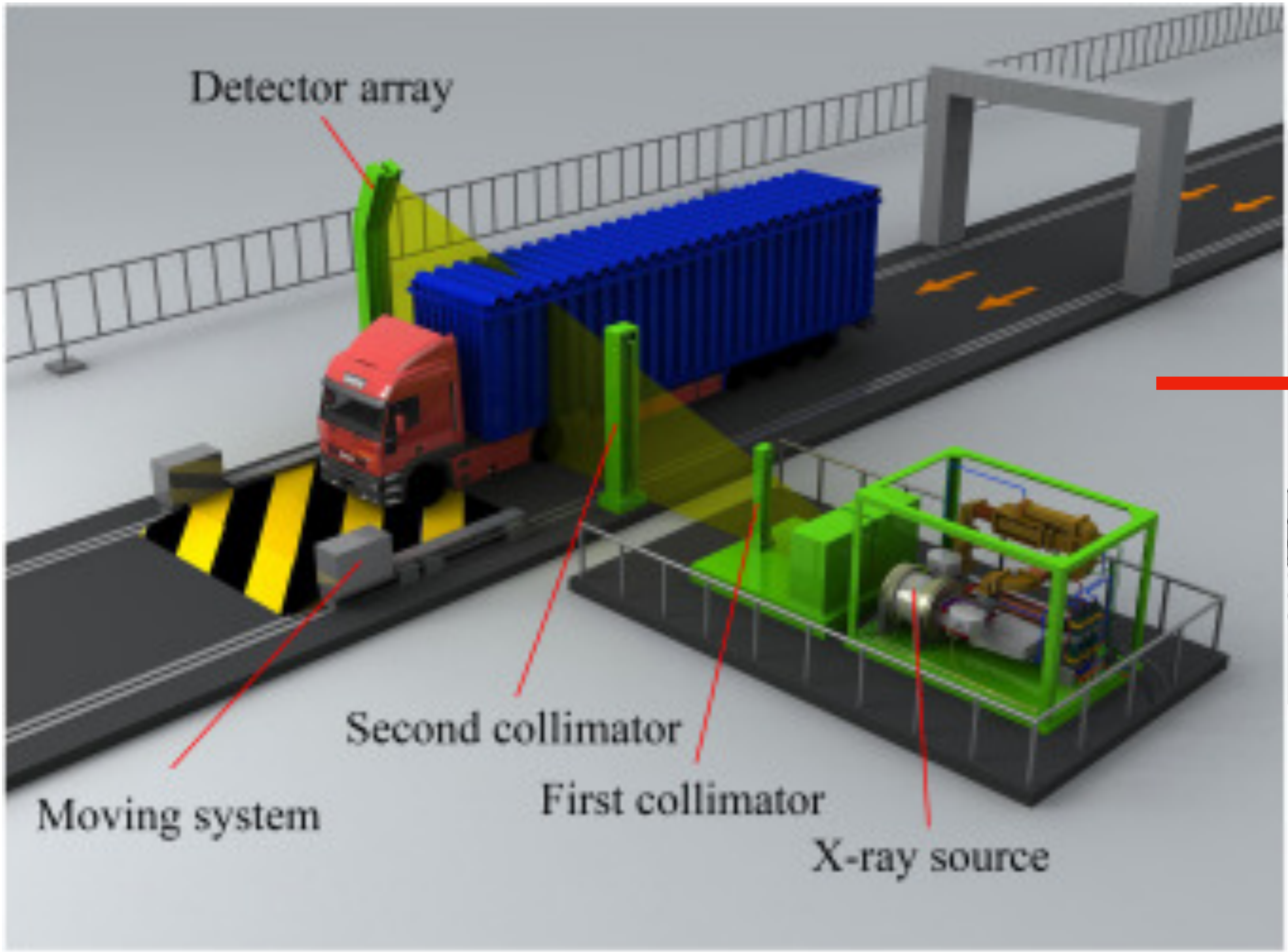

Lee, 2018

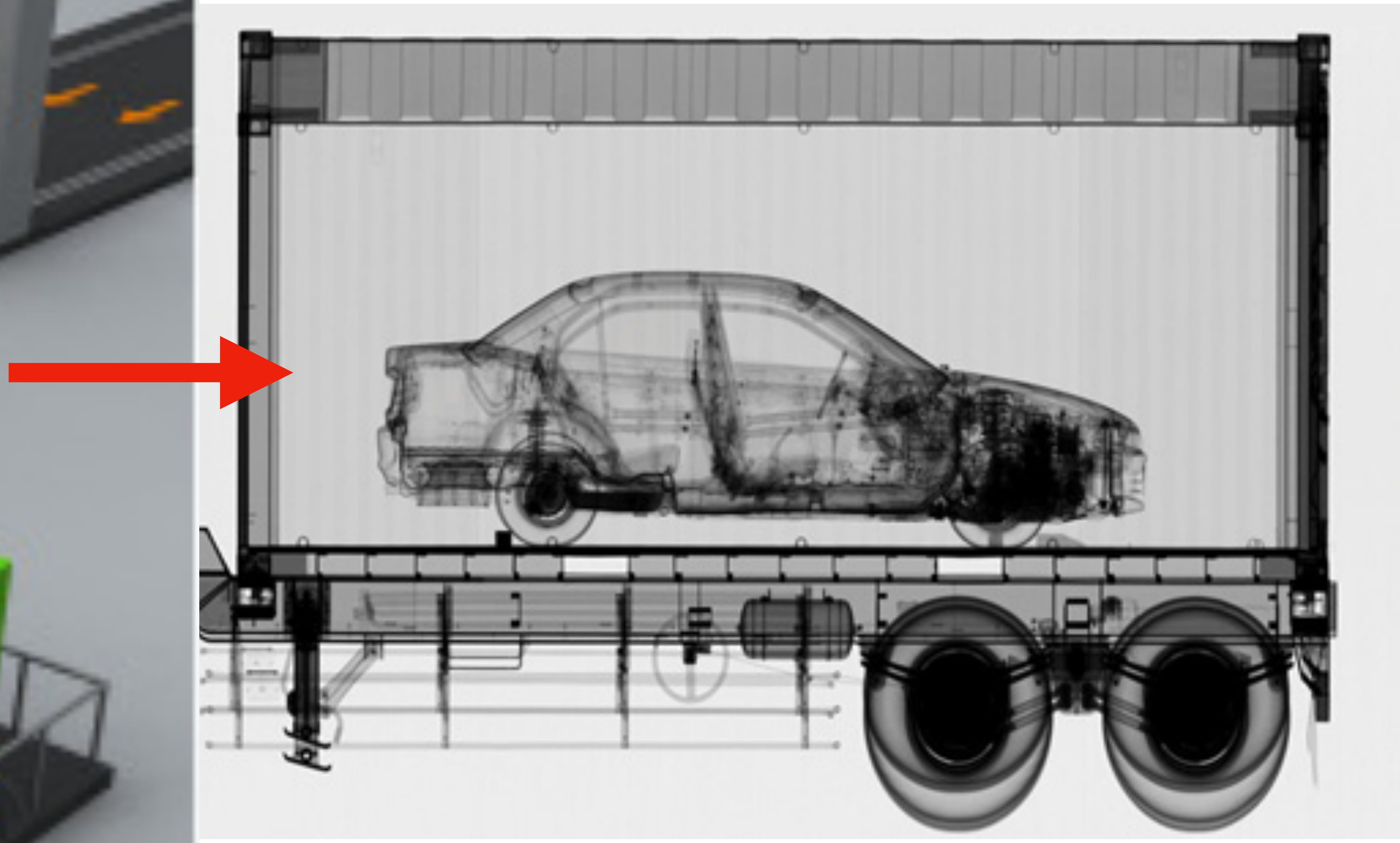

Clements, 2010

How do these scanners work?

Photons pass through a cargo container, where they are attenuated

Linear accelerator generates a Bremsstrahlung photon beam

Detectors measure the transparency T of the beam

$T = 1 \implies$ no attenuation
$T = 0 \implies$ total attenuation

Dual energy systems enable material identification

rapiscansystems.com

- The photon beam transparency depends on:
  - **area density** (λ)
  - **atomic number** (Z)
- **Idea:** perform two separate measurements using different photon energies
  - $T_H :=$ high energy transparency
  - $T_L :=$ low energy transparency
- **Result:** system of two equations and two unknowns

Current methods use calibration scans to generate lookup databases


Linac

Calibration Material

Detector

Interlaced {high, low} energy beams

	$Z = 6$	$Z = 13$	$Z = 26$	$Z = 82$
$\lambda = 5\ \mathrm{g/cm^2}$	$T_H = 0.828$ $T_L = 0.784$	$T_H = 0.812$ $T_L = 0.769$	$\dots$	$\dots$
$\lambda = 10\ \mathrm{g/cm^2}$	$T_H = 0.692$ $T_L = 0.622$	$T_H = 0.666$ $T_L = 0.599$	$\dots$	$\dots$
$\lambda = 15\ \mathrm{g/cm^2}$	$\dots$	$\dots$	$\dots$	$\dots$
$\lambda = 20\ \mathrm{g/cm^2}$	$\dots$	$\dots$	$\dots$	$\dots$
$\lambda = 25\ \mathrm{g/cm^2}$	$\dots$	$\dots$	$\dots$	$\dots$
$\lambda = 30\ \mathrm{g/cm^2}$	$\dots$	$\dots$	$\dots$	$\dots$
$\lambda = 35\ \mathrm{g/cm^2}$	$\dots$	$\dots$	$\dots$	$\dots$
$\lambda = 40\ \mathrm{g/cm^2}$	$\dots$	$\dots$	$\dots$	$\dots$
$\vdots$	$\dots$	$\dots$	$\dots$	$\dots$

Material classification is performed by reference to these databases

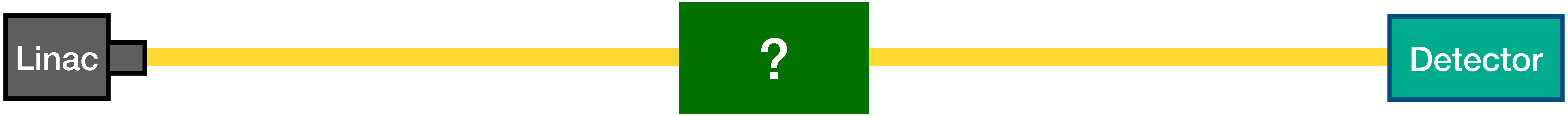

$T_H = 0.302$
$T_L = 0.242$

Interlaced {high, low} energy beams

	$Z = 6$	$Z = 13$	$Z = 26$	$Z = 82$
$\lambda = 5\ \mathrm{g/cm^2}$	$T_H = 0.828$ $T_L = 0.784$	$T_H = 0.812$ $T_L = 0.769$	$\ldots$	$\ldots$
$\lambda = 10\ \mathrm{g/cm^2}$	$T_H = 0.692$ $T_L = 0.622$	$T_H = 0.666$ $T_L = 0.599$	$\ldots$	$\ldots$
$\lambda = 15\ \mathrm{g/cm^2}$	$\ldots$	$\ldots$	$\ldots$	$\ldots$
$\lambda = 20\ \mathrm{g/cm^2}$	$\ldots$	$\ldots$	$\ldots$	$\ldots$
$\lambda = 25\ \mathrm{g/cm^2}$	$\ldots$	$\ldots$	$\ldots$	$\ldots$
$\lambda = 30\ \mathrm{g/cm^2}$	$\ldots$	$\ldots$	$\ldots$	$\ldots$
$\lambda = 35\ \mathrm{g/cm^2}$	$\ldots$	$\ldots$	$\ldots$	$\ldots$
$\lambda = 40\ \mathrm{g/cm^2}$	$\ldots$	$\ldots$	$\ldots$	$\ldots$
$\vdots$	$\ldots$	$\ldots$	$\ldots$	$\ldots$

Material classification is performed by reference to these databases

$T_H = 0.302$
$T_L = 0.242$

Interlaced {high, low} energy beams

	$Z = 6$	$Z = 13$	$Z = 26$	$Z = 82$
$\lambda = 5\ \mathrm{g/cm^2}$	$T_H = 0.828$ $T_L = 0.784$	$T_H = 0.812$ $T_L = 0.769$	$\dots$	$\dots$
$\lambda = 10\ \mathrm{g/cm^2}$	$T_H = 0.692$ $T_L = 0.622$	$T_H = 0.666$ $T_L = 0.599$	$\dots$	$\dots$
$\lambda = 15\ \mathrm{g/cm^2}$	$\dots$	$\dots$	$\dots$	$\dots$
$\lambda = 20\ \mathrm{g/cm^2}$	$\dots$	$\dots$	$\dots$	$\dots$
$\lambda = 25\ \mathrm{g/cm^2}$	$\dots$	$\dots$	$\dots$	$\dots$
$\lambda = 30\ \mathrm{g/cm^2}$	$\dots$	$\dots$	$\dots$	$\dots$
$\lambda = 35\ \mathrm{g/cm^2}$	$\dots$	$\dots$	$\dots$	$\dots$
$\lambda = 40\ \mathrm{g/cm^2}$	$\dots$	$\dots$	$\dots$	$\dots$
$\vdots$	$\dots$	$\dots$	$\dots$	$\dots$

This approach has obvious downsides

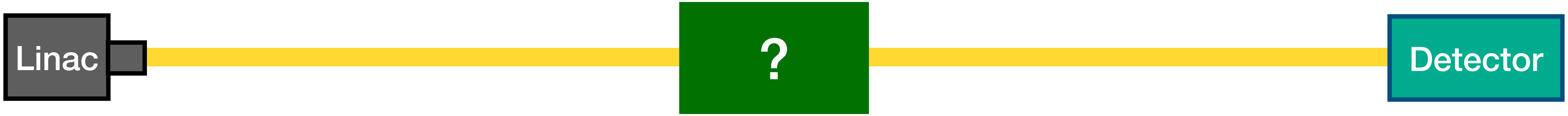

Interlaced {high, low} energy beams

	$Z = 6$	$Z = 13$	$Z = 26$	$Z = 82$
$\lambda = 5\ \mathrm{g/cm^2}$	$T_H = 0.828$ $T_L = 0.784$	$T_H = 0.812$ $T_L = 0.769$	$\ldots$	$\ldots$
$\lambda = 10\ \mathrm{g/cm^2}$	$T_H = 0.692$ $T_L = 0.622$	$T_H = 0.666$ $T_L = 0.599$	$\ldots$	$\ldots$
$\lambda = 15\ \mathrm{g/cm^2}$	$\ldots$	$\ldots$	$\ldots$	$\ldots$
$\lambda = 20\ \mathrm{g/cm^2}$	$\ldots$	$\ldots$	$\ldots$	$\ldots$
$\lambda = 25\ \mathrm{g/cm^2}$	$\ldots$	$\ldots$	$\ldots$	$\ldots$
$\lambda = 30\ \mathrm{g/cm^2}$	$\ldots$	$\ldots$	$\ldots$	$\ldots$
$\lambda = 35\ \mathrm{g/cm^2}$	$\ldots$	$\ldots$	$\ldots$	$\ldots$
$\lambda = 40\ \mathrm{g/cm^2}$	$\ldots$	$\ldots$	$\ldots$	$\ldots$
$\vdots$	$\ldots$	$\ldots$	$\ldots$	$\ldots$

- **Requires a lot of calibration data**
- **Unclear how to extrapolate to elements which are not included during calibration step**

Other methods invert an analytic transparency model

$$T = \frac{\text{Detected charge in the presence of a material}}{\text{Detected charge without any intervening material}}$$

Detected charge $=$ # of original photons $\times$ probability photon reaches detector $\times$ detected charge per photon

Determine
from beam
simulations

$$e^{-\mu(E,Z)\lambda}$$

Calculate from
detector response
simulations

$\mu(E,Z) =$ mass attenuation coefficient
for element Z at photon energy E

Combine it all together: $$T(\lambda, Z) = \frac{\int_0^\infty D(E)\phi(E)e^{-\mu(E,Z)\lambda}dE}{\int_0^\infty D(E)\phi(E)dE}$$

where $D(E)$ is the detector response function and $\phi(E)$ is the photon energy spectrum

However, the analytic model is not perfect

- Errorbars show simulation output
- Dashed lines show model predictions
- Each element forms a different line
- **An inaccurate transparency model will result in incorrect material predictions**

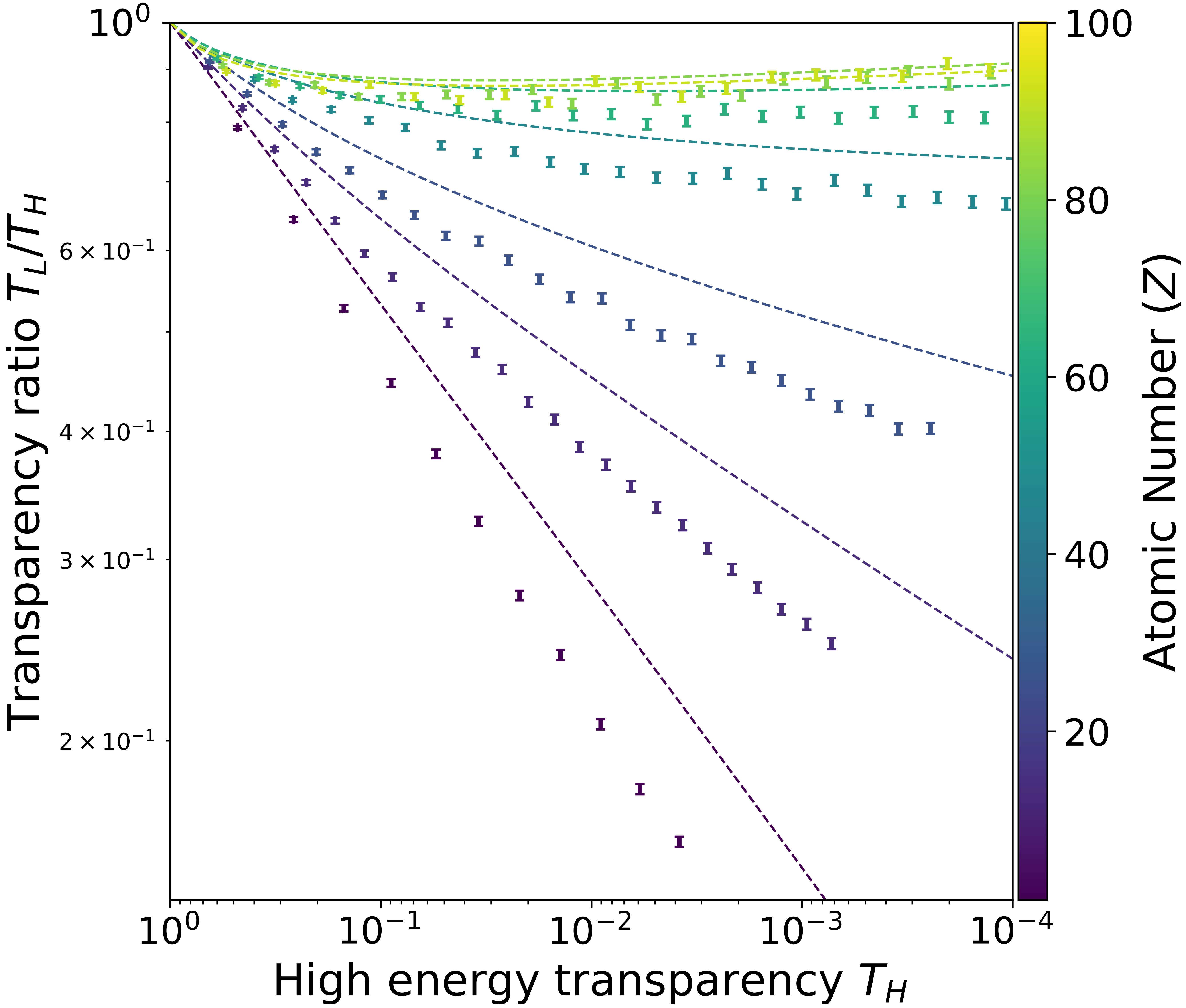

This work: improving the analytic model

- **Can we use empirical data to tweak the analytic model?**

- Expand the mass attenuation coefficient in terms of the photoelectric effect (PE), Compton scattering (CS), and pair production (PP):

$$\mu(E,Z) = \mu_{\text{PE}}(E,Z) + \mu_{\text{CS}}(E,Z) + \mu_{\text{PP}}(E,Z)$$

- Define a semiempirical mass attenuation coefficient, $\tilde{\mu}(E,Z;a,b,c)$, as follows:

$$\tilde{\mu}(E,Z;a,b,c) = a\mu_{\text{PE}}(E,Z) + b\mu_{\text{CS}}(E,Z) + c\mu_{\text{PP}}(E,Z)$$

Calculate a, b, and c through a simple calibration procedure

The semiempirical model shows improved accuracy

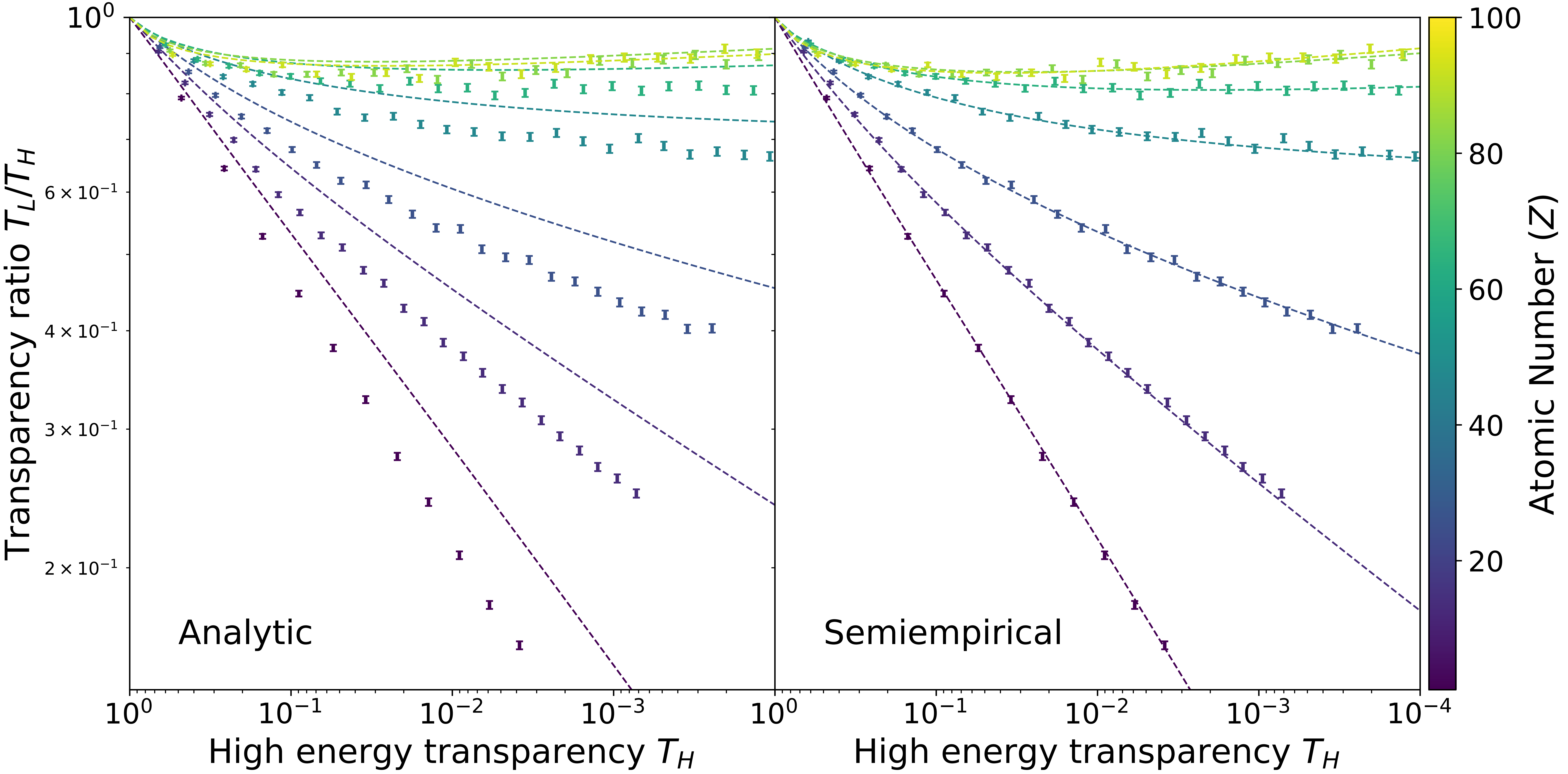

Validating the model using simulated radiographs

- Insert different materials inside a steel container

- Run beam transparency simulations using Geant4

- Can we reconstruct the materials?

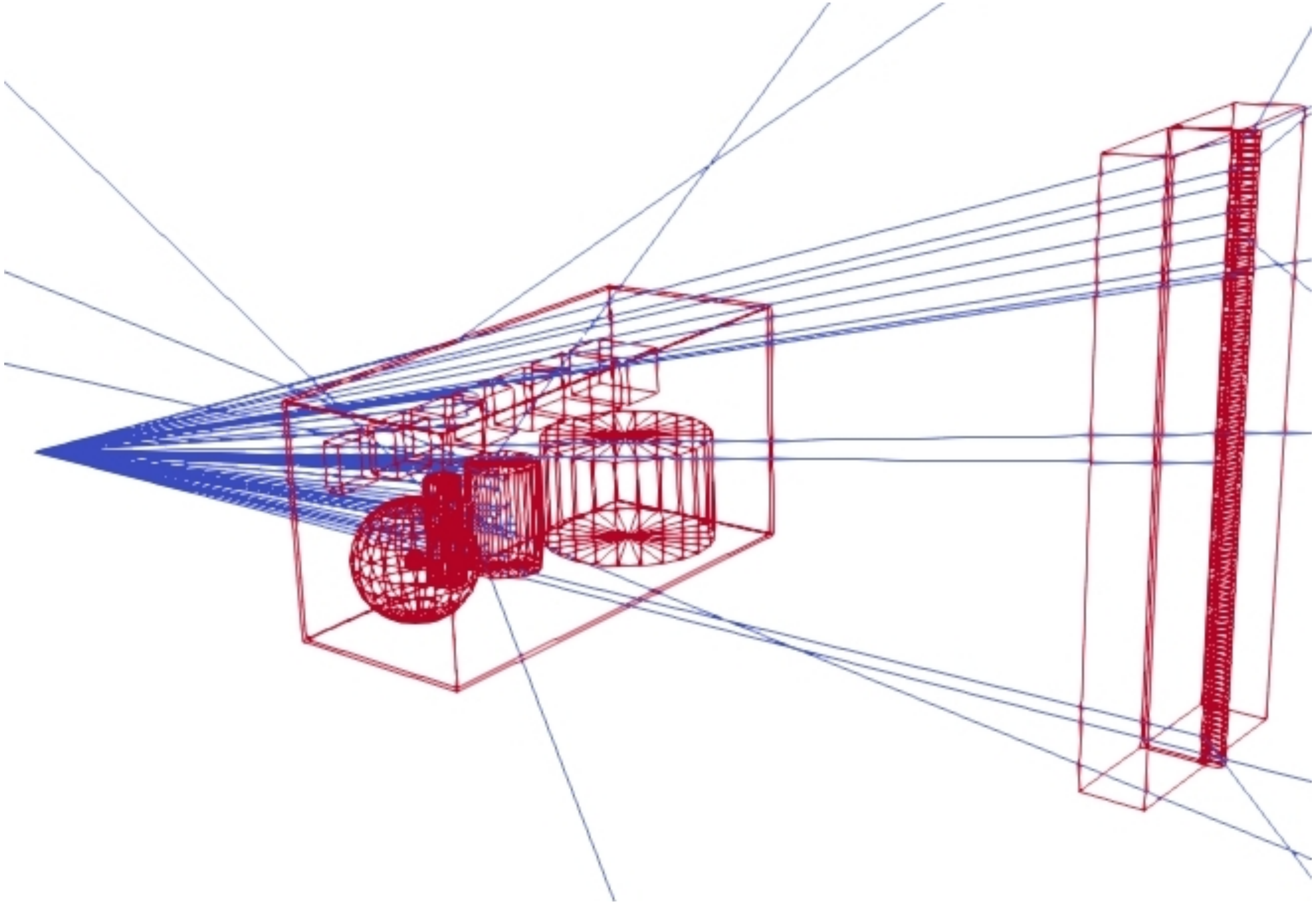

The importance of high-performance computing

- Typical flux of ~10 million photons per second per detector
- Container is moving $\Longrightarrow$ different simulations for every vertical slice
- Access to HPC resources has been essential for obtaining high resolution simulations

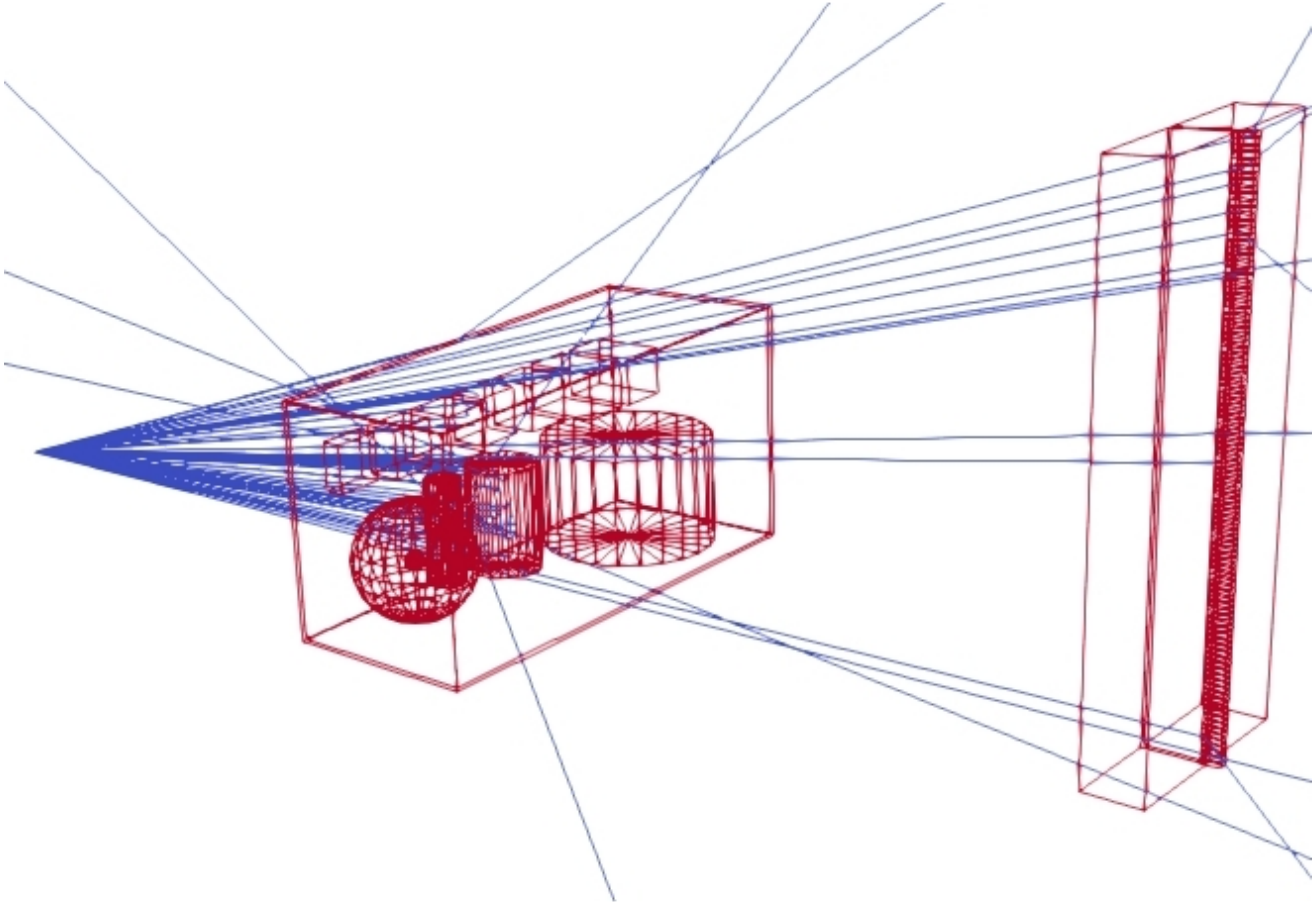

The atomic number reconstruction algorithm

1. Segment the image into different regions

2. Define a chi-squared loss function

$$\chi^2 = \sum_{\text{all pixels}} \frac{(\text{predicted} - \text{observed})^2}{\text{uncertainty}^2}$$

3. For each region, find the value of Z which minimizes χ^2

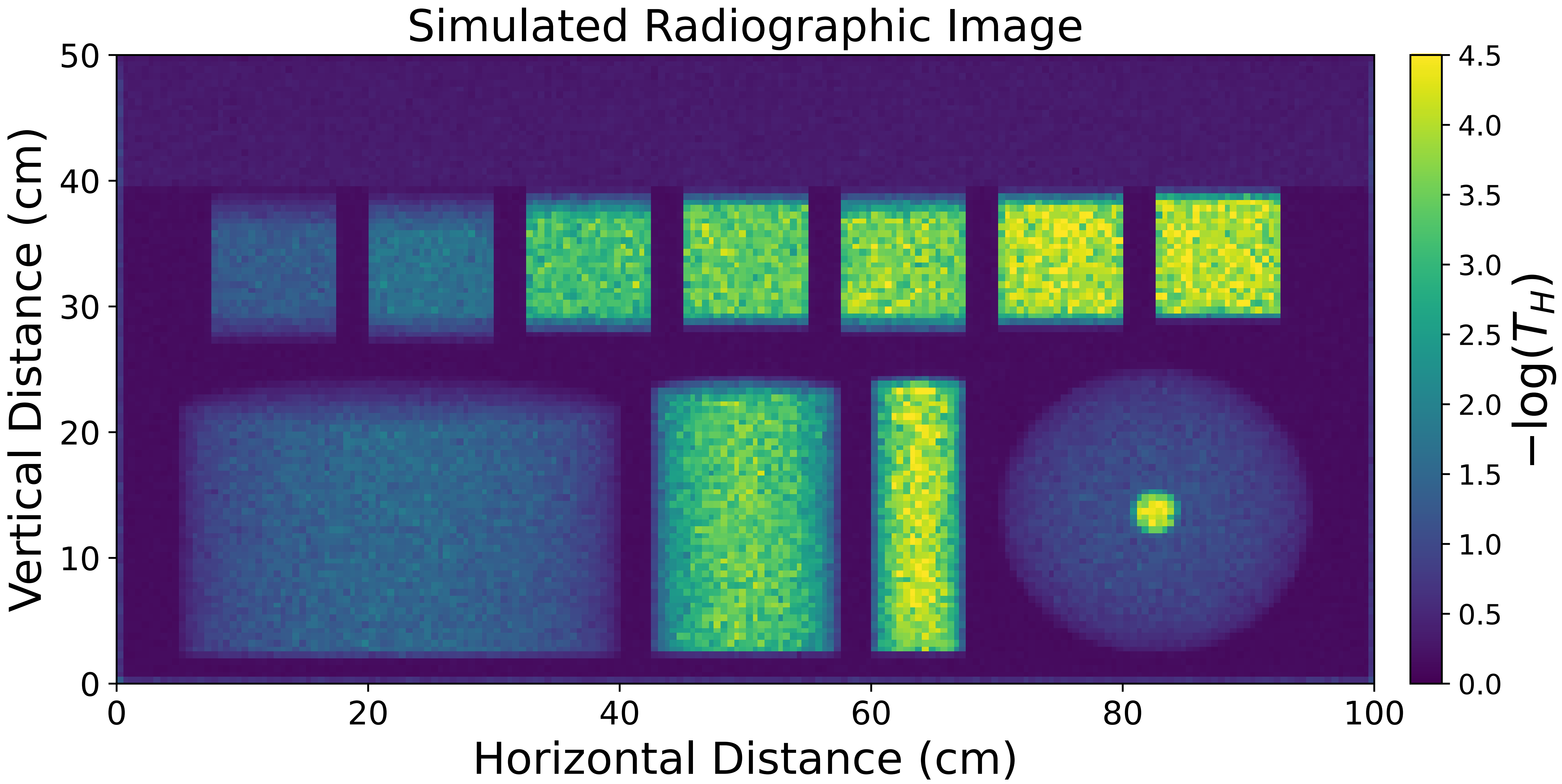

Algorithm performs well on simulated image

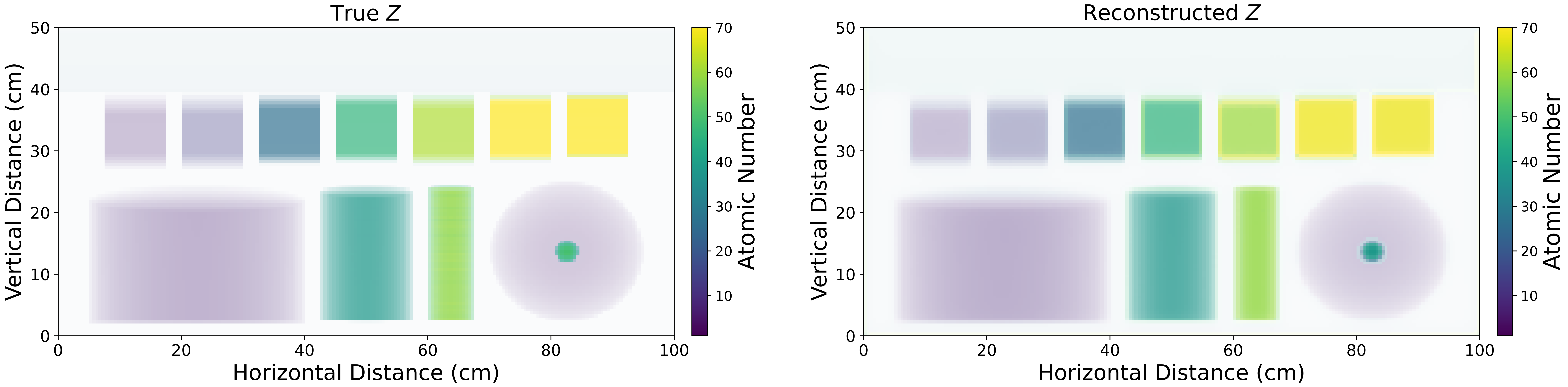

Uncertainty Estimation

Methodology

1. Generate 1000 noisy simulation images
2. Run Z reconstruction algorithm on each image
3. Calculate variation amongst different Z estimates

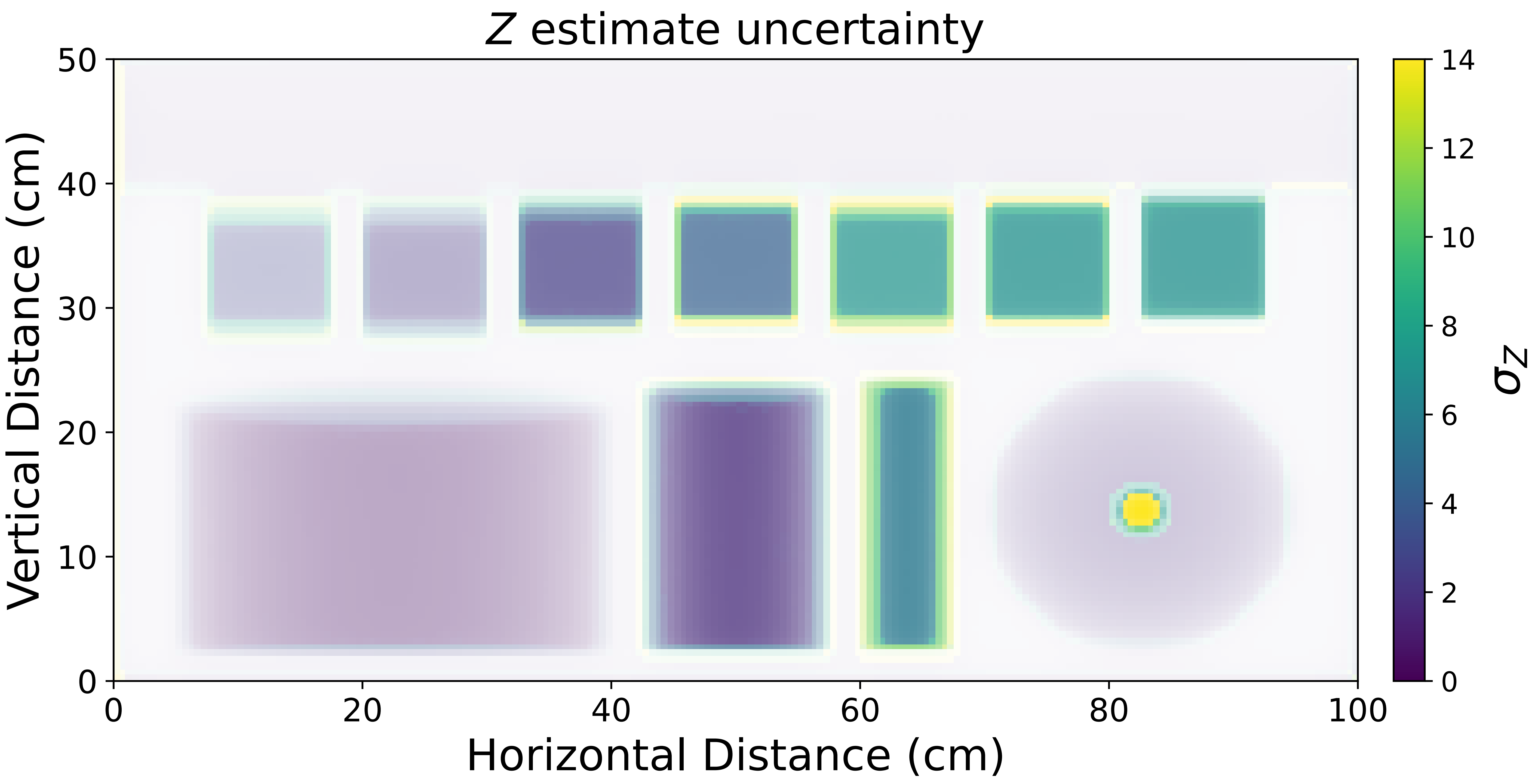

Uncertainty estimate is smaller than bin sizes of prior work

Conclusions

- This work presents a fast and accurate method for reconstructing the atomic number of X-ray images
- Predicting the Z of every pixel can assist port operators in identification of illicit materials
- Method was validated against simulated radiographic images, enabled by access to HPC resources
- Extended applications beyond the scope of this talk, such as calculating the Z of materials which are hidden behind shielding